Biochemical Pharmacology 104 (2016) 74–82

Contents lists available at ScienceDirect

Biochemical Pharmacology

journal homepage: www.elsevier.com/locate/biochempharm

Porcine lactoferrin-derived peptide LFP-20 protects intestinal barrier by maintaining tight junction complex and modulating inflammatory response

Xin Zong, Wangyang Hu, Deguang Song, Zhi Li, Huahua Du, Zeqing Lu, Yizhen Wang *

Key Laboratory of Animal Nutrition and Feed Science in Eastern China, Ministry of Agriculture, College of Animal Sciences, Zhejiang University, Hangzhou 310058, China

ARTICLE INFO

Article history:
Received 11 November 2015
Accepted 13 January 2016
Available online 14 January 2016

Keywords:
LFP-20
Intestinal barrier
Tight junction
Inflammation
NF-κB

ABSTRACT

LFP-20, a 20-amino acid antimicrobial peptide in the N terminus of porcine lactoferrin, has antimicrobial and immunomodulatory activities. This study assessed the protective effects of LFP-20 on LPS-induced intestinal damage in a LPS-induced mouse model and *in vitro*, using intestinal porcine epithelial cell line 1 (IPEC-1) cells. LFP-20 prevented LPS-induced impairment in colon epithelium tissues, infiltration of macrophages or leukocytes, histological evidence of inflammation and increased levels of TNF-a, IL-6 and IFN-γ. LFP-20 increased the expression of zonula occludens-1, occludin and claudin-1 and reduced permeability as well as apoptosis of the colon in LPS-treated mice. In IPEC-1 cells, LFP-20 increased transepithelial electrical resistance and tight junction expression. Moreover, we found LFP-20 decreased the MyD88 and AKT levels to affect the NF-κB signaling pathway, to modulate inflammation response and tight junction networks in the processing of LPS stimulation. In summary, LFP-20 prevents the inflammatory response and disruption of tight junction structure induced by LPS, suggesting the potential use of LFP-20 as a prophylactic agent to protect intestinal barrier function.

1. Introduction

The intestinal mucosa forms a physical and metabolic barrier against the diffusion of pathogens, toxins and allergens from the lumen into the circulatory system [1]. Compromising the barrier function of the intestinal mucosa increases host susceptibility to luminal antigens and pathogens, followed by chronic response of the intestinal immune system [2]. It is also a major contributing factor in the pathogenesis of inflammatory bowel diseases (IBD), such as Crohn's disease and ulcerative colitis [3]. Although the pathogenesis of IBD has not been entirely elucidated yet, it is known that the activation of inflammation and relapses of some diseases are relevant to natural and adaptive immune responses, such as the overproduction of TNF-α and IFN-γ in the intestine [4]. These proinflammatory cytokines potentially impair mucosal barrier function and intestinal permeability [5].

Several mechanisms are involved in proinflammatory cytokine-induced disruption in the intestinal mucosa, including down-regulation of the expression of tight junction (TJ) proteins [1,6]. The formation of TJs in epithelial cells serves as a pivotal section of the intestinal barrier. The TJ complexes consist of epithelial cells and intercellular junctions [7]. To date, a variety of protein components of TJs have been identified, such as occludins, claudins and zonula occludens (zo)-1 [8]. Both claudins and occludins are coupled either directly or indirectly to cytoskeleton actin filaments with zo-1 and other factors [9]. Considerable evidence suggests that maintaining tight junction networks benefits some gastrointestinal diseases, including IBD [10,11].

NF-κB is a transcription factor that plays an important role in the regulation of gene expression associated with many cellular processes. When NF-κB is activated, IκBs, inhibitory proteins of NF-κB, are phosphorylated by IKK, thereby allowing activated NF-κB to translocate into the nucleus [12]. Increasing evidence indicates that inflammatory diseases involve the overexpression of pro-inflammatory cytokines, such as TNF-α, IL-6 and IL-1β, via NF-κB pathways [13]. Activated NF-κB may bind to the myosin light chain kinase (MLCK) promoter region and increase MLCK expression [14]. MLCK-mediated MLC phosphorylation has been found to result in the contraction of actin–myosin filaments, altering TJ protein localization and expression as well as TJ barrier functional openings [15]. These findings suggest that NF-κB plays a crucial role in intestinal barrier damage and inflammation response in IBD.

* Corresponding author at: Institute of Feed Science, Zhejiang University, 866 Yuhangtang Road, Hangzhou 310058, China.
E-mail address: yzwang321@zju.edu.cn (Y. Wang).

http://dx.doi.org/10.1016/j.bcp.2016.01.009
0006-2952/

Peptide fragments isolated from the degradation of lactoferrins (LFs) displayed higher antimicrobial activity than their native protein counterparts [16,17]. LFP-20 is one of the 20 amino acid antimicrobial peptides identified in the N terminus of LF, which is a member of the porcine LF family [18]. LFP-20 shows antimicrobial effects on *Escherichia coli*, *Staphylococcus aureus* and *Candida albicans* [19]. Our previous study identified key amino acids in the LFP-20 sequence using amino acid substitutions and activity assays [20] and suggested that LFP-20 attenuated inflammation is associated with MyD88/NF-κB and MyD88/MAPK signaling pathways [18]. Many studies have confirmed the relationship of inflammation to barrier function, but the effects of LFP-20 on intestinal barrier function and its underlying mechanism have not been elucidated.

This study investigated the protective effects of LFP-20 on the epithelial barrier. LFP-20 was administered intraperitoneally to mice and a parallel treatment starting together with LPS. The protective effects and the molecular basis of action of LFP-20 were investigated by assessing alterations in the integrity of the intestinal barrier and the innate immune response to LPS challenge.

2. Materials and methods

2.1. Peptide synthesis

LFP-20 (KCRQWQSKIRRTNPIFCIRR) was chemically synthesized by GL Biochem (Shanghai) Ltd, achieving 98% purity of the synthetic peptide. The peptide was dissolved in endotoxin-free water and stored at −80 °C.

2.2. Animal model

Seventy-two C57/BL6 male mice (6–8 weeks of age) were obtained from the Laboratory Animal Center of Zhejiang University (Hangzhou, China) and maintained in plastic cages under standard conditions. All animals were provided with food and water *ad libitum* during the experimental period (1 week). The animal experimental protocols were approved by the Animal Care and Use Committee of Zhejiang University.

The mice were randomly divided into six groups of 12 each: control, LFP-20 treatment, LPS treatment, 2.5 mg/kg LFP-20 pretreatment followed by LPS treatment (LFPL + LPS), 5 mg/kg LFP-20 pretreatment followed by LPS treatment (LFPM + LPS) and 10 mg/kg LFP-20 pretreatment followed by LPS treatment (LFPH + LPS). The different concentrations of LFP-20 were injected intraperitoneally once daily for 6 days, whereas the control and LPS-treated groups were intraperitoneally injected with an equal volume of sterile saline. On day 6, mice in LPS and LFP-20 (12.5, 25 and 50 μg/ml) + LPS groups were intraperitoneally injected with LPS (10 mg/kg mouse weight) 1 h after LFP-20 or saline treatment, and the other groups were injected with an equal volume of saline. All mice were euthanized by cervical dislocation 6 h after i.p. injection of LPS or saline, and tissues and blood were collected [18].

2.3. Cell culture

Intestinal porcine epithelial cell line 1 (IPEC-1) cells were purchased from the CBCAS (Cell Bank of the Chinese Academy of Sciences, Shanghai, PR China) and cultured in DMEM F12 medium (Gibco) supplemented with 10% (v/v) fetal bovine serum (Hyclone) and antibiotics (100 U/ml penicillin and 100 μg/ml streptomycin sulfate) (Hyclone) at 37 °C in a fully humidified incubator under 5% CO_2 in air.

2.4. Histopathology and immunohistochemistry

Intestinal tissues of the colon were fixed in 4% paraformaldehyde solution immediately after the mice were euthanized. Tissues were embedded in paraffin and cut into 5-mm-thick sections. For the evaluation of histopathology changes, the tissues were stained with hematoxylin–eosin (H&E) and observed under a microscope (Leica NEWDM 4500BR). Histopathological changes were graded on the histological injury scale described by Jang et al. [21].

For the immunohistochemical analysis of CD68, anti-CD68 antibodies (Santa, USA) were added at a dilution of 1:100 and incubated overnight at 4 °C after blocking with 1% w/v BSA for 1 h. After washing with PBS, samples were treated with HRP-conjugated rabbit anti-goat IgG (HuaAn, Hangzhou, China) at a ratio of 1:100. Samples were incubated at 4 °C for 1 h and washed with PBS three times. DAB (50–100 μL) (Dako, USA) was added, and the slices were counterstained with hematoxylin. Finally, the samples were dehydrated in an ethanol (70–100%) gradient and treated with xylene to increase the transparency of slides. Neutral balsam was used for mounting.

The cell apoptosis rate in the colon epithelium was determined by TUNEL according to the manufacturer's instructions in situ cell death detection kit (KeyGen BioTECH, Nanjing, China). Healthy and apoptotic cardiomyocytes were counted in four to six randomly selected fields at 200× magnification. The percentage of apoptotic cells was taken as the percentage of the total number of TUNEL-positive cells.

2.5. ELISA and myeloperoxidase (MPO) activity assay

Concentrations of TNF-α, IL-6, IFN-γ and IL-4 in colons were determined using commercial ELISA quantitative kits (eBioscience, San Diego, USA) according to the manufacturer's instructions.

The activities of MPO were assessed by ELISA kits (Boster Wuhan, China) according to the manufacturer's instructions. Results were expressed in U/(mg protein).

2.6. Immunofluorescence analysis of TJ proteins

The expression levels of intercellular tight junction protein zo-1 and occludin were evaluated by immunofluorescence microscopy as previously described [22]. Briefly, IPEC-1 cells were incubated with a mouse monoclonal anti-zo-1 Ab and an anti-occludin Ab (Abcam, USA) and then with DyLight 488-conjugated secondary Ab. After washing with PBS, the cells were incubated in a medium containing 40 mg/ml DAPI and examined with a Leica fluorescence microscope (Keyence, Osaka, Japan).

2.7. Intercellular tight junctions observed by transmission electron microscopy (TEM)

The tight junctions between gut epithelial cells were characterized by TEM. For TEM assessment, a colon specimen of approximately 1 cm in length was excised with a sharp scalpel and fixed in 2.5% glutaraldehyde for 4 h at 4 °C, followed by fixation in osmic acid and embedding in epon. Ultrathin sections were obtained using a diamond knife and stained with uranyl acetate and lead citrate before examination by TEM (JEM-1011; JEOL USA). Digital electron micrographs were acquired with a 1024 × 1024 pixel CCD camera system (AMT Corp., Denver, MA) [23].

2.8. Measurement of transepithelial electrical resistance (TEER)

IPEC-1 cells were grown on 12-mm Transwell® filters (Corning Incorporated, Corning, NY, USA). TEER was determined with an Evom^2 epithelial voltohmmeter according to the manufacturer's

instructions, and background resistance was determined using cell-free filters. Cells were untreated or incubated with 1 μg/ml LPS pretreated with 25 μg/ml LFP-20 or not, LPS and LFP-20 were added into the upper chamber. Measurements were performed at different times (0.5, 1, 2, 4, 8, 12 and 24 h), background was subtracted and changes were calculated as a percentage of baseline TEER. Experiments were performed in triplicate [24].

Electrophysiological parameters were measured with a multichannel voltage/current clamp (VCC MC6; Physiologic Instruments). Ussing chambers were equipped with two pairs of Ag/AgCl electrodes connected to the chambers via 3 M KCl/3.5% agar bridges. After equilibration for 30 min, basal electrical readings of potential difference (PD), Isc and total electrical resistance (RT) were obtained every 15 min for 2 h. RT was calculated using Ohm's law, where PD = Isc × RT [25].

2.9. Western blot analysis

Whole protein was obtained with a whole protein extraction kit (KeyGEN Biotech, Nanjing, China) according to the manufacturer's instructions. Protein concentrations were determined with the BCA assay kit (KeyGEN Biotech, Nanjing, China). Next, 40 μg of total protein of each specimen was separated by 10% SDS–PAGE and transferred onto polyvinylidene difluoride membranes (PVDF). The membranes were then blocked with 5% nonfat dried milk proteins in 0.05% TBST and probed with MyD88, IKK-β, p-IKK-β, IκB-α, p-IκB-α, NF-κB, p-NF-κB, AKT, p-AKT and β-actin-specific monoclonal antibodies. After washing with TBST, proteins were detected with HRP-conjugated secondary antibodies (HuaAn, Hangzhou China) for 1 h. Specific bands were visualized with an ECL detection kit (Santa Cruz Biotechnology, Inc., CA, USA) [18].

2.10. Data analysis

Statistical tests were performed using GraphPad Prism version 5.01 (GraphPad Software, Inc., San Diego, CA, USA) by one-way analysis of variance and post hoc analysis by Duncan's test. Data are presented as mean ± SEM. An alpha value of $p < 0.05$ was considered statistically significant.

2.11. Materials

Ultrapure LPS from *E. coli* strain O111:B4 was purchased from Sigma–Aldrich (St. Louis. MO, USA). Rabbit anti-zo-1 and anti-occludin polyclonal antibodies were purchased from Abcam (Abcam, Cambridge, MA, USA). Mouse monoclonal antibodies MyD88, IκB-α, p-IκB-α, NF-κB, NF-κB, AKT, p-AKT or β-actin were obtained from Santa Cruz Biotechnology (Santa Cruz, CA, USA). IKK-β and p-IKK-β were purchased from Cell Signaling Technology (MA, USA). The IgG-HRP secondary antibodies were purchased from HuaAn (Hangzhou, China).

3. Results

3.1. LFP-20 prevented LPS-induced impairment of colon epithelium tissues

As expected, LPS damaged the colon's mucosal barrier, leading to gut inflammation and weight loss. Treatment with LFP-20

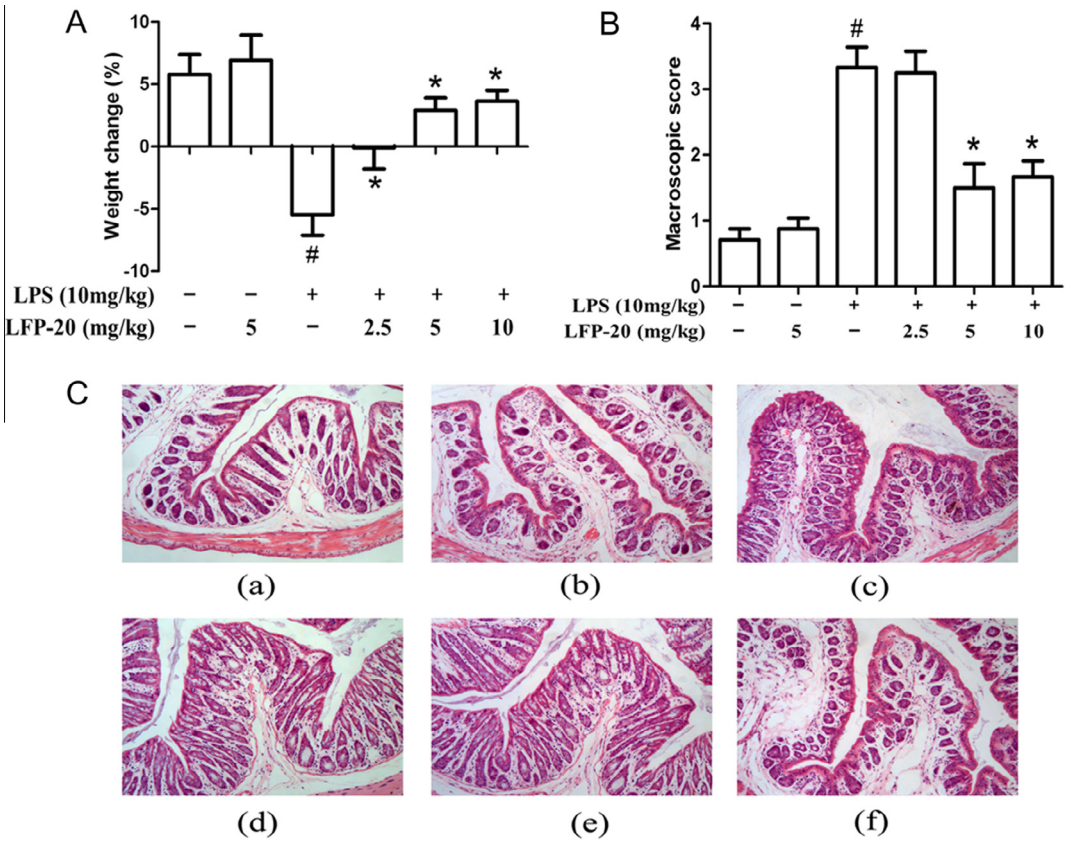

Fig. 1. The protective effects of LFP-20 against LPS-stimulated mouse on clinical symptoms. Protective effect of LFP-20 on body weight (A), macroscopic disease (B). Representative H&E-stained section from (C-a) control, (C-b) LFP-20, (C-c) LPS, (C-d) LFPL + LPS, (C-e) LFPM + LPS, (C-f) LFPH + LPS. Original magnification 200×. Results are given as mean ± SEM. Differences between groups were determined by one-way ANOVA followed by Duncan's post hoc analysis ($n = 12$). $^{\#}p < 0.05$ as compared to the control group, and $^{*}p < 0.05$ as compared to the LPS-treated group.

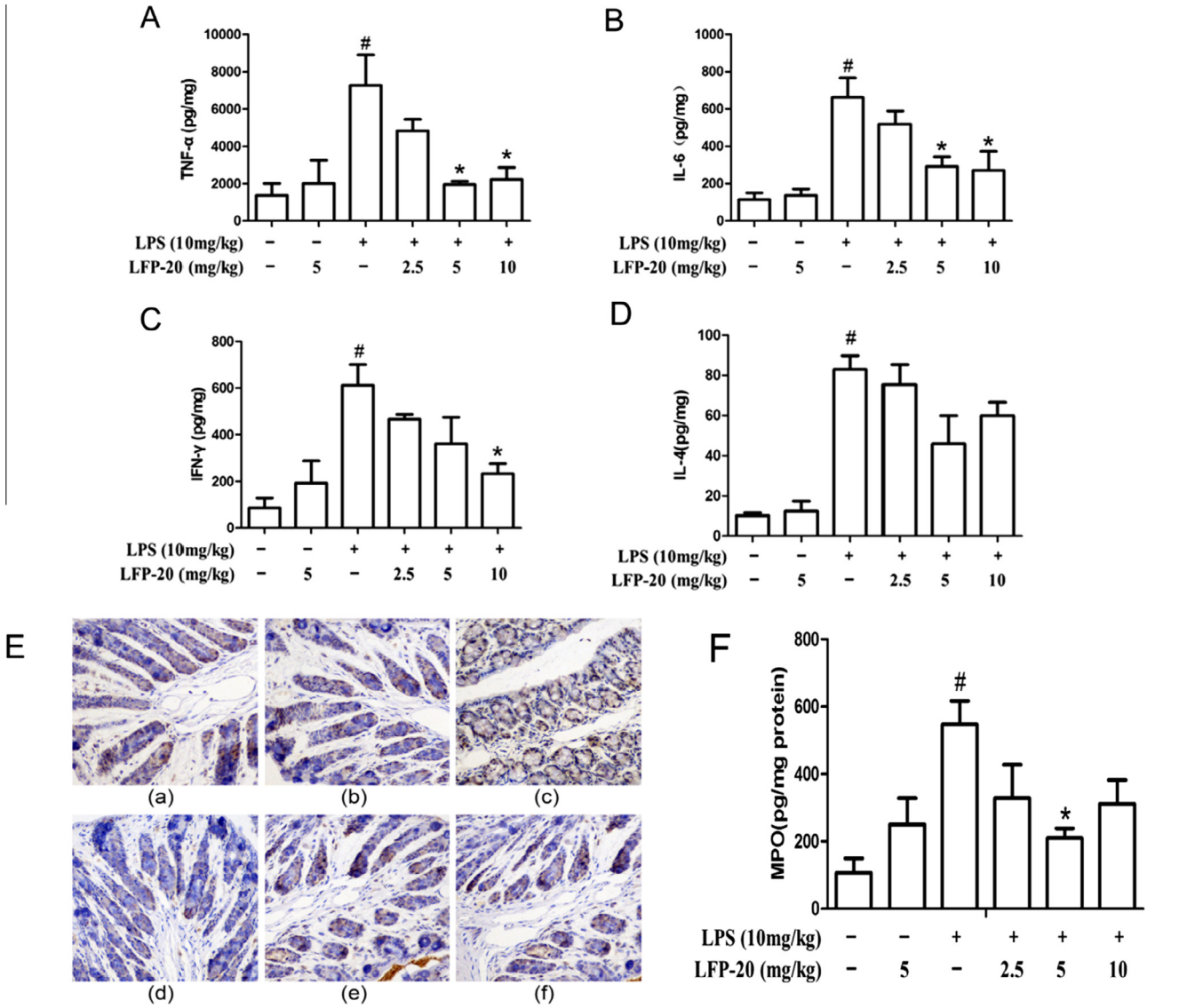

Fig. 2. The protective effects of LFP-20 on inflammatory response. ELISA for TNF-α (A), IL-6 (B), IFN-γ (C) and IL-4 (D) in colonic tissues. Representative images of the CD68 cells (E). Original magnification, 400×. Formalin-fixed, paraffin-embedded 5-mm cross-sections were stained with a primary Ab to CD68. (E-a) control, (E-b) LFP-20, (E-c) LPS, (E-d) LFPL + LPS, (E-e) LFPM + LPS, (E-f) LFPH + LPS. Enzymatic activities of MPO were measured (F). Results are given as mean ± SEM. Differences between groups were determined by one-way ANOVA followed by Duncan's post hoc analysis ($n = 12$). $^{\#}p < 0.05$ as compared to the control group, and $^{*}p < 0.05$ as compared to the LPS-treated group.

resulted in prominent protection from LPS-induced damage, as assessed by body weight, macroscopic score (Fig. 1A and B) and histopathological damage to the colon (Fig. 1C). In contrast to the LPS-treated group, which showed significant weight loss compared with the control group, mice in the LFP-20-pretreated group showed little body weight loss (Fig. 1A). These protective effects were confirmed by macroscopic examination of the colon (Fig. 1B).

Histological examination of colon tissue from the LPS-induced group revealed considerable tissue injury with extensive ulceration of the epithelial layer, edema, crypt damage to the bowel wall and infiltration of granulocytes and mononuclear cells into the mucosa (Fig. 1C). In contrast, LFP-20 pretreatment reduced the histological evidence of LPS-induced colon damage.

To characterize the protective effects of LFP-20 against inflammation in LPS-stimulated mice, inflammatory markers were detected by Elisa, including TNF-α, IL-6, IFN-γ and IL-4. As shown in Fig. 2A–D, the secretion of TNF-α, IL-6, IFN-γ and IL-4 in the LPS-treated group were significantly greater than those in the LFP-20-pretreated group. MPO (an indicator of colonic infiltration with polymorphonuclear leukocytes) activity in colon tissue from LPS treated mice was markedly increased compared with control mice, whereas LFP-20 pretreated groups showed significantly decreased MPO activities compared with the LPS-treated group (Fig. 2F).

The infiltration of CD68 cells into colonic tissue was detected by immunohistochemistry. In contrast to minimal infiltration of macrophages into the colons of control mice, we observed increased infiltration of CD68 macrophages into the colonic lesion area (Fig. 2E). Pretreatment with LFP-20 reduced the infiltration of macrophages compared with the group treated with LPS alone (Fig. 2E).

TUNEL staining of the sections of colon tissue was performed to identify alterations in the level of apoptosis. The results showed that the apoptosis level (brown signals) of the LPS-treated group was higher than that of the control group, as quantified by the apoptosis index (Fig. 3). Compared with the LPS-treated group,

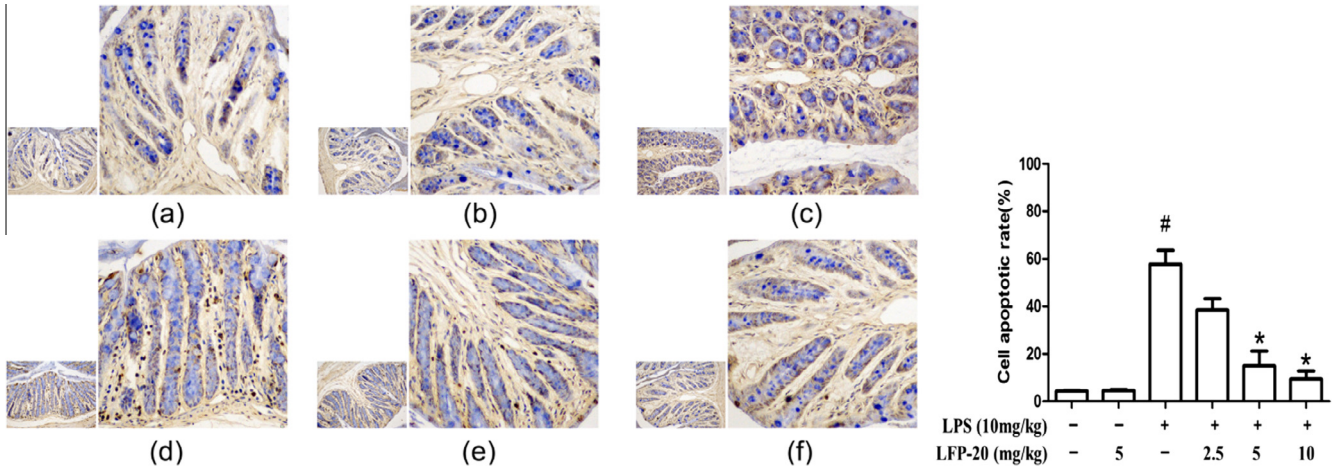

Fig. 3. TUNEL staining of colon epithelial tissues. (a) Control, (b) LFP-20, (c) LPS, (d) LFPL + LPS, (e) LFPM + LPS, (f) LFPH + LPS. The images were analyzed with at least four views of each image taken under 400× magnification. Five random duplications in each group were analyzed, and the number of apoptotic cells counted according to the positive color of brown and the average calculated. Results are given as mean ± SEM. Differences between groups were determined by one-way ANOVA followed by Duncan's post hoc analysis ($n = 6$). $^{\#}p < 0.05$ as compared to the control group, and $^{*}p < 0.05$ as compared to the LPS-treated group.

pretreatment with 5 and 10 mg/kg LFP-20 in LPS-administered mice significantly reduced the apoptosis index by 42.8% and 48.6% ($p < 0.5$) respectively (Fig. 3). The apoptosis indexes in mice treated with LFP alone were similar to that of the control group.

3.2. LFP-20 prevented the LPS-induced disruption of intestinal TJ structure and function

To investigate the protective effects of LFP-20 on the LPS-induced disruption of TJs, TJ markers, such as claudin-1, occludin and zo-1, were determined by Western blotting. TJ marker expression were down-regulated in mice treated with LPS alone, compared with normal animals (Fig. 4A). The expression of these TJ markers in pretreatment with LFP-20 groups was significantly higher than that in the LPS group treated alone (Fig. 4A), suggesting the importance of LFP-20 for maintaining the integrity of the junction complex. Consistently, the tight junctions between gut epithelial cells were confirmed by TEM, with the results also supporting the protective effect of LFP-20 against LPS-induced damage in colon tissue (Fig. 5).

To evaluate the functional integrity of mouse intestinal epithelium under *ex vivo* conditions, TEER measurements were performed for 60 min. As shown in Fig. 4B, compared with the control group, the TEER values in the LPS-treated group declined significantly, indicating an increase in permeability. In contrast, pretreatment with different concentrations of LFP-20 resulted in a significant protective effect, especially in the 5- and 10-mg/kg LFP-20-treated groups. These results confirmed the role of LFP-20 activation in minimizing LPS-induced intestinal epithelial hyperpermeability (Fig. 4B).

3.3. LFP-20 effects on NF-κB signaling pathway in LPS-stimulated mice

To investigate whether NF-κB is involved in the pathway through which LFP-20 regulates inflammatory and barrier function, we evaluated the phosphorylation status of NF-κB and

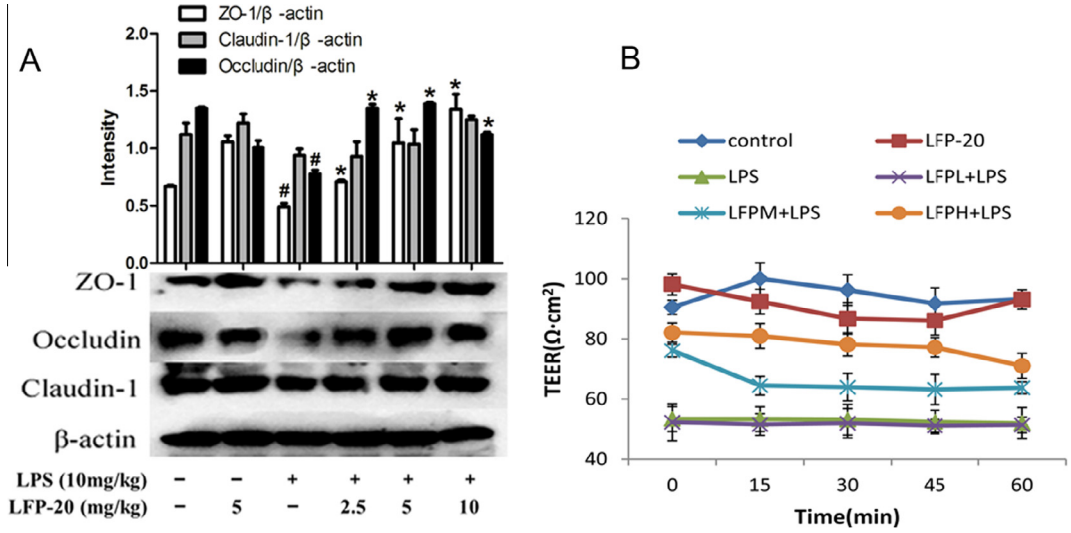

Fig. 4. The protective effects of LFP-20 on intestinal barrier. (A) Expression of TJ proteins were determined by Western-blot. (B) TEER of mouse colonic epithelium measured ex *vivo* in Ussing chambers. Results are given as mean ± SEM. Differences between groups were determined by one-way ANOVA followed by Duncan's post hoc analysis ($n = 6$). $^{\#}p < 0.05$ as compared to the control group, and $^{*}p < 0.05$ as compared to the LPS-treated group.

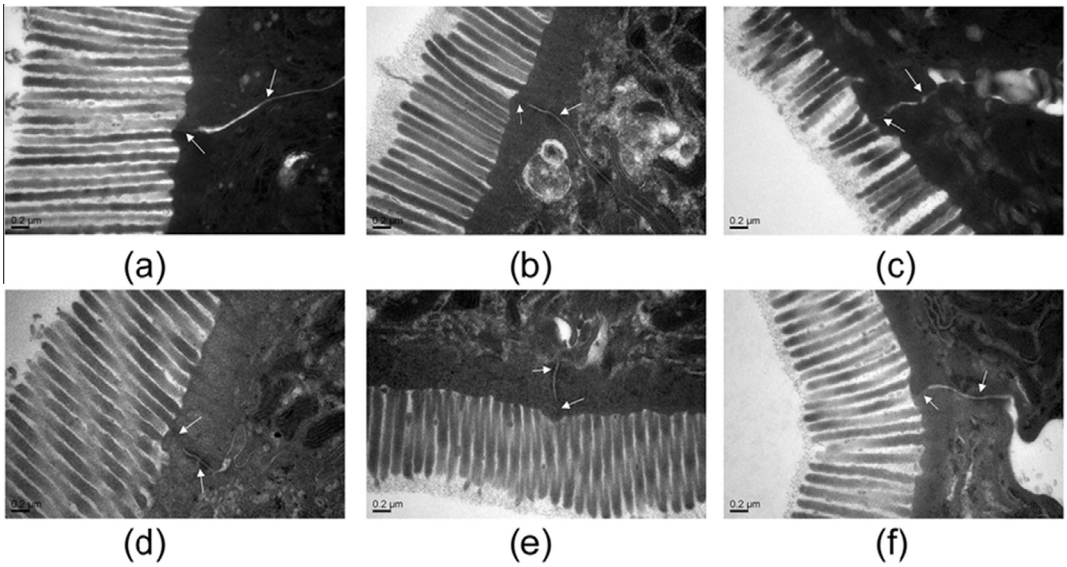

Fig. 5. The protective effects of LFP-20 on intestinal TJs structure. TJs structure of colonic epithelium were determined by transmission electron microscope (TEM), under 50,000× magnification, (a) control, (b) LFP-20, (c) LPS, (d) LFPL + LPS, (e) LFPM + LPS, (f) LFPH + LPS, the wider intervals (white arrowheads) between the intestinal epithelial cells were indicated.

IκB-α. The amount of p-NF-κB increased significantly after stimulation with LPS. Pretreatment with various concentrations of LFP-20 reversed the increase in a dose-dependent manner (Fig. 6B). To further characterize the effects of LFP-20, we examined intracellular effectors upstream of NF-κB, such as IKK-β, AKT and MyD88. As expected, pretreatment with various concentrations of LFP-20 effectively inhibited the phosphorylation of AKT and MyD88, which is activated by LPS stimulation (Fig. 6A). However, the suppressive effect of LFP-20 on IKK-β was negligible (Fig. 6A). These results indicated that the activation of NF-κB plays a crucial role in the process of LFP-20 modulating the inflammation and barrier in mice stimulated by LPS.

3.4. The protective effects of LFP-20 on the structure and function of the junction complexes in LPS-induced IPEC-1 cells

To determine whether LFP-20 could prevent LPS-induced reduction in TJ expression *in vitro*, Western-blot analysis was performed for the expression levels of TJ markers. LPS significantly reduced the expression of zo-1, claudin-1 and occludin compared with control, but the expression of TJ markers in the LFP-20 pretreatment groups was significantly higher than that in the LPS-alone group (Fig. 7A). Consistently, LFP-20 exposure was associated with a disturbed and irregular cellular distribution of zo-1 and occludin compared with the control IPEC-1 cells (Fig. 7C). The control group pretreated with 5 mg/kg LFP-20 showed no effects on the zo-1 and occludin cellular distribution, whereas LPS derangement of the distribution of zo-1 and occludin appeared to be prevented by LFP-20 (Fig. 7C).

To further characterize the protective role of LFP-20 in LPS-induced damage to intestinal barrier function, we performed a TEER assay using the IPEC-1 cell culture system. TEER values rapidly decreased by 1 h in LPS treated cells. However, in LFP-20 pretreated cells, the average TEER value moderately decreased by 1 h (Fig. 7B) and increased by 4 h, reaching 80% of the baseline value.

3.5. NF-κB activation is involved in the protective effects of LFP-20 in IPEC-1 cells

To confirm the mechanism of LFP-20 in modulating inflammation and barrier in mice stimulated by LPS, we investigated the MyD88/AKT/NF-κB signaling pathway in LPS-stimulated IPEC-1 cells pretreated with LFP-20 or not. Compared with the control group, the phosphorylation of MyD88, AKT, NF-κB and IκB-α was markedly increased in LPS-treated IPEC-1 cells, and the amounts of these proteins decreased in the group pretreated with LFP-20 (Fig. 8). Although the change in the expression of phosphorylation of IKK-β was not as evident as the phosphorylation of MyD88, AKT, NF-κB and IκB-α, the regulation effect of LFP-20 on IKK-β was in good agreement with the corresponding changes in their levels.

4. Discussion

The gastrointestinal tract, generally considered as a digestive and absorptive organ, can also function as a barrier againwst pathogens in the lumen [26]. A massive number of pathogenic bacteria colonizes the gastrointestinal tract and may cause intestinal ischemia leading to deterioration of the intestinal epithelial barrier [27]. The integrity of the epithelial barrier is vital for maintaining mucosal homeostasis against gastrointestinal disorder [26,28]. Although the etiology and pathogenesis of chronic inflammatory bowel diseases require more profound investigation, the symptoms have already been characterized as excessive secretion of cytokines and epithelial barrier dysfunction [29,30]. Some studies have shown that pro-inflammatory cytokines play an important role in the process of barrier dysfunction [31,32]. This study focused on assessment of the protective effects of LFP-20 on the LPS-induced intestinal damage in *in vitro* models and an *in vivo* study in mice.

Murine models of intestinal inflammation have been widely used to investigate the regulatory mechanisms, which participate in the reduction of inflammation and restoration of intestinal homeostasis. In this study, we showed that LFP-20 treatment could improve wet weight and reduce histological damage induced by LPS in the intestine. To identify the mechanisms of observed beneficial effects of LFP-20 on LPS-stimulated mice, the anti-inflammatory activity of LFP-20 was assayed. Infiltration of activated macrophages is one of the most representative histological features of intestinal inflammation because they produce superoxide anions and other reactive species [33]. Our findings showed that infiltration of activated macrophages was markedly increased in LPS-treated mice and that pre-treatment with LFP-20 reduced

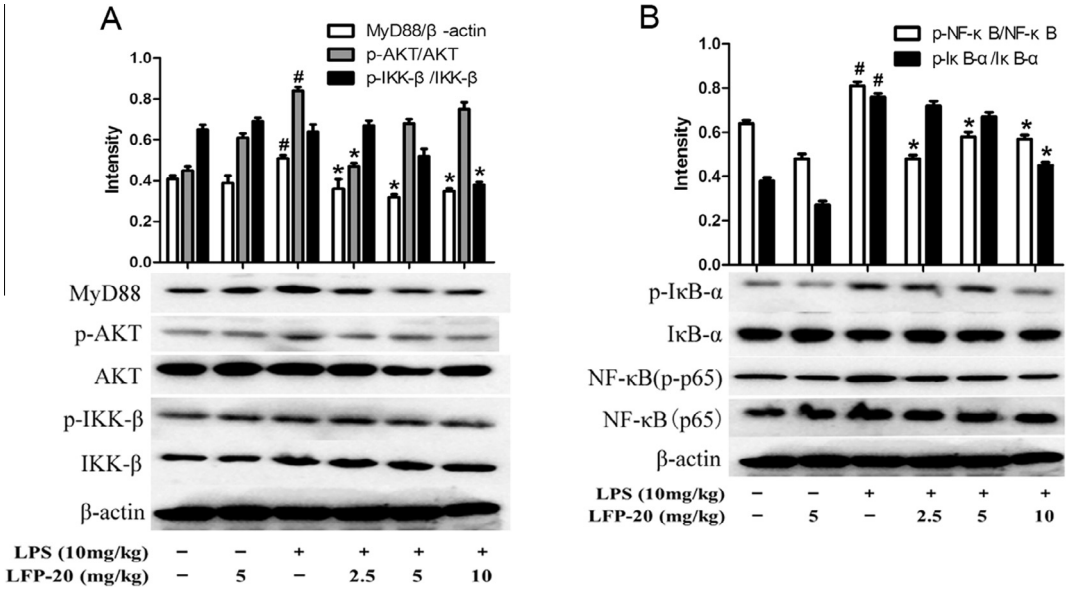

Fig. 6. Inhibitory effect of LFP-20 on the NF-κB signaling pathways *in vivo*. Phosphorylated and total protein levels of MyD88, AKT and IKK-β (A), NF-κB and IκB-α (B) and β-actin from colon epithelial tissues were determined using Abs recognizing phospho-specific or total protein. Results are given as mean ± SEM. Differences between groups were determined by one-way ANOVA followed by Duncan's post hoc analysis ($n = 3$). $^{\#}p < 0.05$ as compared to the control group, and $^{*}p < 0.05$ as compared to the LPS-treated group.

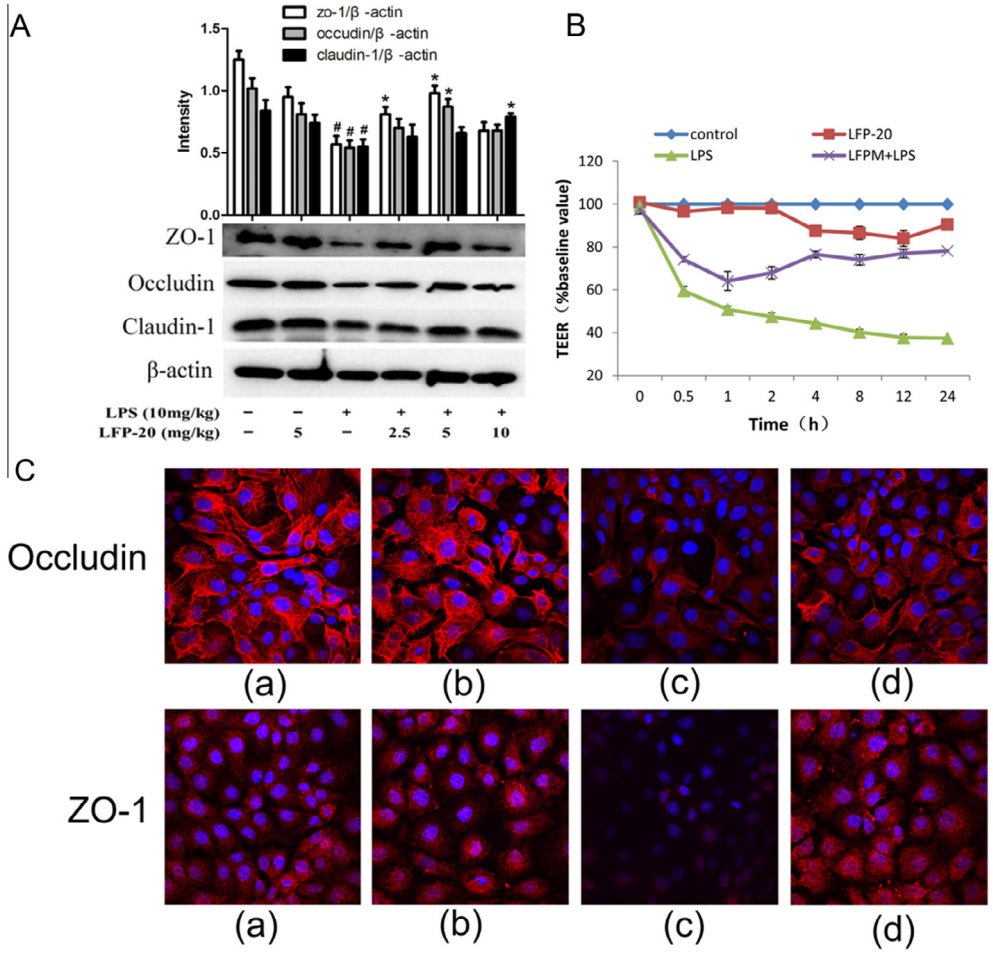

Fig. 7. The protective effects of LFP-20 on intestinal TJs structure and function *in vitro*. (A) Expression of TJ proteins were assessed by Western-blot. (B) Protective effects of LFP-20 (25 μg/ml) on TEER of a IPEC-1 cell monolayer stimulated by LPS (1 μg/ml). (C) Visualization of the zo-1 and occludin expression in IPEC-1 cell monolayer (shown in red) and its combination with DAPI to visualize the nuclei (shown in blue). (C-a) control, (C-b) LFP-20, (C-c) LPS, (C-d) LFPM + LPS. These are representative pictures of three independent experiments. IPEC-1 cells were incubated with 1 μg/ml LPS pretreated with 25 μg/ml LFP-20 or not. Results are given as mean ± SEM. Differences between groups were determined by one-way ANOVA followed by Duncan's post hoc analysis ($n = 3$). $^{\#}p < 0.05$ as compared to the control group, and $^{*}p < 0.05$ as compared to the LPS-treated group. (For interpretation of the references to colour in this figure legend, the reader is referred to the web version of this article.)

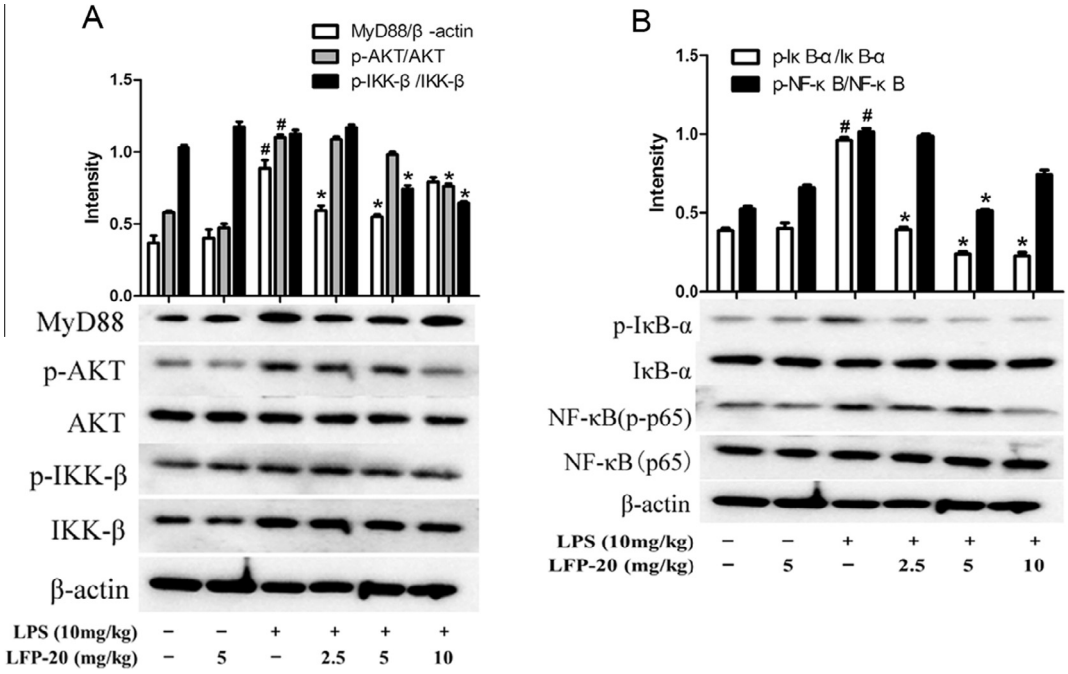

Fig. 8. Inhibitory effect of LFP-20 on the NF-κB signaling pathways in LPS-stimulated IPEC-1 cells. IPEC-1 cells were incubated with 1 μg/ml LPS pretreated with 25 μg/ml LFP-20 or not. Phosphorylated and total protein levels of MyD88, AKT and IKK-β (A), NF-κB and Iκ B-α (B) and β-actin were determined using Abs recognizing phospho-specific or total protein. Results are given as mean ± SEM. Differences between groups were determined by one-way ANOVA followed by Duncan's post hoc analysis ($n = 3$). $^{\#}p < 0.05$ as compared to the control group, and $^{*}p < 0.05$ as compared to the LPS-treated group.

this effect. MPO activity is directly proportional to neutrophil concentration in the inflamed tissue and is thus an index of neutrophil infiltration and inflammation [34]. Consistently, the results indicated that MPO activity was also significantly reduced in LFP-20 pretreated mice.

IBD is involved in excessive generation of inflammatory cytokines, such as tumor necrosis factor-α (TNF-α), which can amplify the inflammatory cascade by triggering the production of other pro-inflammatory cytokines and enhancing the accumulation and activation of leukocytes [35]. The finding that pretreatment with LFP-20 reduced the levels of TNF-α, IL-6 and IFN-γ in the colon suggests that LFP-20 ameliorates LPS-induced IBD via the suppression of pro-inflammatory mediators, such as TNF-α, IL-6 and IFN-γ. Increasing evidence suggests that pro-inflammatory cytokines act as a pathophysiologically important regulator affecting the intestinal epithelial tight junction permeability [5,36]. A decrease in cytokine production may promote the recovery of epithelial barrier function [37]. Thus, the decrease in pro-inflammatory cytokines and macrophage invasion in LPS-induced mice treated with LFP-20 may play a role not only in anti-inflammatory but also in epithelial barrier function.

We evaluated the effect of LFP-20 on gut epithelial barrier function *in vivo* and *in vitro*. Our results showed that LFP-20 alleviated LPS-induced permeability by increasing TER values. The barrier regulates macromolecule trafficking between the lumen and internal milieu and protects the host by preventing harmful solutes, microorganisms, toxins and luminal antigens from impairing the body defence mechanism [2]. The intestinal barrier is formed by the interplay of various barrier components, such as intercellular TJ proteins [1]. TJs are capable of restraining paracellular movement of compounds across the intestinal mucosa [38,39]. Increased permeability in TJ may provide a major site for both infection and the establishment of inflammation in the gut [40,41]. Our results showed that the expressions of three major TJ proteins (occludin, claudin-1 and zo-1) were regulated by LFP-20. The effects of LFP-20 on the epithelial barrier could thus be mediated by maintaining the expression of TJs, thereby reducing the severity of gut inflammation.

Much evidence indicates that pro-inflammatory cytokines, such as TNF-α and IL-6, are regulated through the NF-κB pathway [42]. Our previous study showed that treatment with LFP-20 has the potential to directly influence MyD88 levels by blocking its interactions with other signaling molecules in activated macrophages [18]. In this study, Western blot assay suggested that pretreatment with LFP-20 *in vivo* or *in vitro* inhibited the activation of phosphorylation of NF-κB. The activation of MyD88 and IKK-β, upstream proteins of NF-κB, was also inhibited. These results suggest that the anti-inflammatory effects of LFP-20 are linked with the down-regulation of NF-κB in LPS-stimulated mice. However, some studies [43,44] have indicated that tight junction assembly is impaired by the down-regulation of AMPK activity. AMPK plays a crucial role in the balance of cellular energy [45]. It also protects the TJ proteins via the suppression of ROS production, which can cause barrier dysfunction induced by lipopolysaccharide [46].

In conclusion, our study confirms that the protective effects of porcine lactoferricin-derived peptide LFP-20 on the intestinal barrier in LPS-stimulated models may be associated with the maintenance of a tight junction network and the response of modulating inflammation via MyD88/NF-κB signal transduction pathways. As a result, it is able to modulate TJ proteins (occludin, claudin-1 and zo-1) and inhibit the production of inflammation mediators (such as TNF-a, IFN-γ and IL-6). Our results suggest that porcine lactoferricin-derived peptide LFP-20 could serve as a potential prophylactic agent to protect intestinal barrier function when treated with endotoxemia.

Acknowledgements

This work was supported by the National Natural Science Foundation of China (31172213) – China and the earmarked fund for Modern Agroindustry Technology Research System (CARS-36) – China.

References

[1] J.R. Turner, Intestinal mucosal barrier function in health and disease, Nat. Rev. Immunol. 9 (2009) 799–809.
[2] E.J. Park, A.B.R. Thomson, M.T. Clandinin, Protection of intestinal occludin tight junction protein by dietary gangliosides in lipopolysaccharide-induced acute inflammation, J. Pediatr. Gastroenterol. Nutr. 50 (2010) 321–328.
[3] Y. Salim Sa, J.D. Soderholm, Importance of disrupted intestinal barrier in inflammatory bowel diseases, Inflamm. Bowel Dis. 17 (2011) 362–381.
[4] P.R. Gibson, Increased gut permeability in Crohn's disease: is TNF the link? Gut 53 (2004) 1724–1725.
[5] M.B. Soyka, P. Wawrzyniak, T. Eiwegger, D. Holzmann, A. Treis, K. Wanke, et al., Defective epithelial barrier in chronic rhinosinusitis: the regulation of tight junctions by IFN-gamma and IL-4, J. Allergy Clin. Immunol. 130 (2012) 1087–1096.
[6] M.A. McGuckin, R. Eri, L.A. Simms, T.H.J. Florin, G. Radford-Smith, Intestinal barrier dysfunction in inflammatory bowel diseases, Inflamm. Bowel Dis. 15 (2009) 100–113.
[7] S. Koch, A. Nusrat, Dynamic regulation of epithelial cell fate and barrier function by intercellular junctions, in: M. Fromm, J.D. Schulzke (Eds.), Molecular Structure and Function of the Tight Junction: From Basic Mechanisms to Clinical Manifestations, 2009, pp. 220–227.
[8] T. Suzuki, H. Hara, Quercetin enhances intestinal barrier function through the assembly of zonnula occludens-2, occludin, and claudin-1 and the expression of claudin-4 in caco-2 cells, J. Nutr. 139 (2009) 965–974.
[9] E.A. Severson, M. Kwon, R.S. Hilgarth, C.A. Parkos, A. Nusrat, Glycogen synthase kinase 3 (GSK-3) influences epithelial barrier function by regulating occludin, claudin-1 and e-cadherin expression, Biochem. Biophys. Res. Commun. 397 (2010) 592–597.
[10] B.S. Ramakrishna, Probiotic-induced changes in the intestinal epithelium: implications in gastrointestinal disease, Trop. Gastroenterol. 30 (2009) 76–85.
[11] S. Fillon, Z.D. Robinson, S.P. Colgan, G.T. Furuta, Epithelial function in eosinophilic gastrointestinal diseases, Immunol. Allergy Clin. North Am. 29 (2009) 171–178.
[12] B.C. Chen, W.W. Lin, PKC- and ERK-dependent activation of I kappa B kinase by lipopolysaccharide in macrophages: enhancement by P2Y receptor-mediated CaMK activation, Br. J. Pharmacol. 134 (2001) 1055–1065.
[13] P.N. Moynagh, The NF-kappaB pathway, J. Cell Sci. 118 (2005) 4589–4592.
[14] R. Al-Sadi, D. Ye, K. Dokladny, T.Y. Ma, Mechanism of IL-1 beta-induced increase in intestinal epithelial tight junction permeability, J. Immunol. 180 (2008) 5653–5661.
[15] H.R. Ranaivo, N. Carusio, R. Wangensteen, P. Ohlmann, C. Loichot, A. Tesse, et al., Protection against endotoxic shock as a consequence of reduced nitrosative stress in MLCK210-null mice, Am. J. Pathol. 170 (2007) 439–446.
[16] W. Bellamy, M. Takase, H. Wakabayashi, K. Kawase, M. Tomita, Antibacterial spectrum of lactoferricin B, a potent bactericidal peptide derived from the N-terminal region of bovine lactoferrin, J. Appl. Bacteriol. 73 (1992) 472–479.
[17] W. Bellamy, H. Wakabayashi, M. Takase, K. Kawase, S. Shimamura, M. Tomita, Killing of candida-albicans by lactoferricin-B, a potent antimicrobial peptide derived from the N-terminal region of bovine lactoferrin, Med. Microbiol. Immunol. 182 (1993) 97–105.
[18] X. Zong, D. Song, T. Wang, X. Xia, W. Hu, F. Han, et al., LFP-20, a porcine lactoferrin peptide, ameliorates LPS-induced inflammation via the MyD88/NF-kappaB and MyD88/MAPK signaling pathways, Dev. Comp. Immunol. 52 (2015) 123–131.
[19] H.L. Chen, C.C. Yen, C.Y. Lu, C.H. Yu, C.M. Chen, Synthetic porcine lactoferricin with a 20-residue peptide exhibits antimicrobial activity against *Escherichia coli*, *Staphylococcus aureus*, and *Candida albicans*, J. Agric. Food Chem. 54 (2006) 3277–3282.
[20] F.F. Han, Y.H. Gao, C. Luan, Y.G. Xie, Y.F. Liu, Y.Z. Wang, Comparing bacterial membrane interactions and antimicrobial activity of porcine lactoferricin-derived peptides, J. Dairy Sci. 96 (2013) 3471–3487.
[21] S.-E. Jang, S.R. Hyam, J.-J. Jeong, M.J. Han, D.-H. Kim, Penta-O-galloyl-beta-D-glucose ameliorates inflammation by inhibiting MyD88/NF-kappa B and MyD88/MAPK signalling pathways, Br. J. Pharmacol. 170 (2013) 1078–1091.
[22] K.A. Donato, M.G. Gareau, Y.J.J. Wang, P.M. Sherman, *Lactobacillus rhamnosus* GG attenuates interferon-gamma and tumour necrosis factor-alpha-induced barrier dysfunction and pro-inflammatory signalling, Microbiology 156 (2010) 3288–3297.
[23] A. Assa, L. Vong, L.J. Pinnell, J. Rautava, N. Avitzur, K.C. Johnson-Henry, et al., Vitamin D deficiency predisposes to adherent-invasive *Escherichia coli*-induced barrier dysfunction and experimental colonic injury, Inflamm. Bowel Dis. 21 (2015) 297–306.
[24] P. Loma, A. Guzman-Aranguez, M.J. Perez de Lara, J. Pintor, Diadenosine tetraphosphate induces tight junction disassembly thus increasing corneal epithelial permeability, Br. J. Pharmacol. 172 (2015) 1045–1058.
[25] H. Chen, Y. Hu, Y. Fang, Z. Djukic, M. Yamamoto, N.J. Shaheen, et al., Nrf2 deficiency impairs the barrier function of mouse oesophageal epithelium, Gut 63 (2014) 711–719.
[26] X. Mu, C. Pan, S. Zheng, Y. Alhamdi, B. Sun, Q. Shi, et al., Protective effects of carbon monoxide-releasing molecule-2 on the barrier function of intestinal epithelial cells, PLoS One 9 (2014).
[27] C. Ince, Microcirculation in distress: a new resuscitation end point?, Crit Care Med. 32 (2004) 1963–1964.
[28] Y. Yue, S. Wu, Z. Li, J. Li, X. Li, J. Xiang, et al., Wild jujube polysaccharides protect against experimental inflammatory bowel disease by enabling enhanced intestinal barrier function, Food Funct. 6 (2015) 2568–2577.
[29] N.A. Hering, M. Fromm, J.-D. Schulzke, Determinants of colonic barrier function in inflammatory bowel disease and potential therapeutics, J. Physiol. 590 (2012) 1035–1044.
[30] A.D. Kostic, R.J. Xavier, D. Gevers, The microbiome in inflammatory bowel disease: current status and the future ahead, Gastroenterology 146 (2014) 1489–1499.
[31] H. Schmitz, M. Fromm, C.J. Bentzel, P. Scholz, K. Detjen, J. Mankertz, et al., Tumor necrosis factor-alpha (TNF alpha) regulates the epithelial barrier in the human intestinal cell line HT-29/B6, J. Cell Sci. 112 (1999) 137–146.
[32] C.T. Capaldo, A.E. Farkas, R.S. Hilgarth, S.M. Krug, M.F. Wolf, J.K. Benedik, et al., Proinflammatory cytokine-induced tight junction remodeling through dynamic self-assembly of claudins, Mol. Biol. Cell 25 (2014) 2710–2719.
[33] E.L.M. Vieira, A.J. Leonel, A.P. Sad, N.R.M. Beltrao, T.F. Costa, T.M.R. Ferreira, et al., Oral administration of sodium butyrate attenuates inflammation and mucosal lesion in experimental acute ulcerative colitis, J. Nutr. Biochem. 23 (2012) 430–436.
[34] S. Choudhary, A. Keshavarzian, S. Yong, M. Wade, S. Bocckino, B.J. Day, et al., Novel antioxidants Zolimid and AEOL11201 ameliorate colitis in rats, Dig. Dis. Sci. 46 (2001) 2222–2230.
[35] T. Hibi, N. Inoue, H. Ogata, M. Naganuma, Introduction and overview: recent advances in the immunotherapy of inflammatory bowel disease, J. Gastroenterol. 38 (2003) 36–42.
[36] C.T. Capaldo, A. Nusrat, Cytokine regulation of tight junctions, Biochim. Biophys. Acta 1788 (2009) 864–871.
[37] S. Maggini, E.S. Wintergerst, S. Beveridge, D.H. Hornig, Selected vitamins and trace elements support immune function by strengthening epithelial barriers and cellular and humoral immune responses, Br. J. Nutr. 98 (2007) S29–S35.
[38] I.C. McCall, A. Betanzos, D.A. Weber, P. Nava, G.W. Miller, C.A. Parkos, Effects of phenol on barrier function of a human intestinal epithelial cell line correlate with altered tight junction protein localization, Toxicol. Appl. Pharmcol. 241 (2009) 61–70.
[39] T. Suzuki, N. Yoshinaga, S. Tanabe, Interleukin-6 (IL-6) regulates claudin-2 expression and tight junction permeability in intestinal epithelium, J. Biol. Chem. 286 (2011) 31263–31271.
[40] N. Oshitani, K. Watanabe, S. Nakamura, Y. Fujiwara, K. Higuchi, T. Arakawa, Dislocation of tight junction proteins without F-actin disruption in inactive Crohn's disease, Int. J. Mol. Med. 15 (2005) 407–410.
[41] H. Qin, Z. Zhang, X. Hang, Y. Jiang, *L. plantarum* prevents enteroinvasive *Escherichia coli*-induced tight junction proteins changes in intestinal epithelial cells, BMC Microbiol. 9 (2009).
[42] D.K. Zhang, L.N. Cheng, X.L. Huang, W. Shi, J.Y. Xiang, H.T. Gan, Tetrandrine ameliorates dextran-sulfate-sodium-induced colitis in mice through inhibition of nuclear factor-kappa B activation, Int. J. Colorectal Dis. 24 (2009) 5–12.
[43] B. Zheng, L.C. Cantley, Regulation of epithelial tight junction assembly and disassembly by AMP-activated protein kinase, Proc. Natl. Acad. Sci. U.S.A. 104 (2007) 819–822.
[44] L. Zhang, J. Li, L.H. Young, M.J. Caplan, AMP-activated protein kinase regulates the assembly of epithelial tight junctions, Proc. Natl. Acad. Sci. U.S.A. 103 (2006) 17272–17277.
[45] M. Scharl, G. Paul, K.E. Barrett, D.F. McCole, AMP-activated protein kinase mediates the interferon-gamma-induced decrease in intestinal epithelial barrier function, J. Biol. Chem. 284 (2009) 27952–27963.
[46] Z. Zhao, J. Hu, X. Gao, H. Liang, Z. Liu, Activation of AMPK attenuates lipopolysaccharide-impaired integrity and function of blood–brain barrier in human brain microvascular endothelial cells, Exp. Mol. Pathol. 97 (2014) 386–392.